On Multidisciplinary Investigations of Dangerous Natural Phenomena in the Azov–Black Sea Basin

V.N. Belokopytov*, V.V. Fomin, A.V. Ingerov

Marine Hydrophysical Institute, Russian Academy of Sciences, Sevastopol, Russian Federation
**e-mail: v.belokopytov@gmail.com*

Certain results of investigating dangerous phenomena and potential natural disasters in the Azov–Black Sea basin are represented. The decrease of storm activity in the Black Sea observed in the end of the XX century is due to diminution of total amount and intensity of the passing cyclones. According to long-term tendencies of the North Atlantic Oscillation and the East Atlantic Oscillation atmosphere indices, future increase of the storm amount in the Black Sea would be expected. The effective sources of storm surges in the Sea of Azov are the atmospheric cyclones spreading with the 20–40 km/h velocity. The decrease of a cyclone movement velocity results in a storm surge intensification in the Gulf of Taganrog and increase of the flooded area in the Don delta. When the Don discharge becomes lower than the threshold value ~1600 m^3/s, the wind surge exerts a blocking impact upon the river water that promotes the sea level rise in the branches and the delta lowland. The highest potential tsunami hazard for the Black Sea northern coast is represented by the earthquake epicenters located in the Crimea – Caucasus seismic zone. Noticeable sea level oscillations can arise in some locations of the Crimea Southern Coast as a result of the trapped waves propagating to the northwest, north and northeast from the seismic centers nearby the southern coast of the sea.

Keywords: storm winds, storm surge, tsunami, numerical modeling, the Black Sea, the Sea of Azov

DOI: 10.22449/1573-160X-2017-3-28-44

Introduction. One of directions of scientific activities towards which S.F. Dotsenko fruitfully worked was the study of natural disasters in the Azov–Black Sea basin. For a long time he led the projects on complex research of different natural phenomena. During these studies a wide variety of methods (from field observation data analysis to the mathematic modeling) was used. Among different types of natural disasters (geophysical, geological, meteorological, hydrological, biological, cosmic, etc.) the catastrophes of hydrometeorological type occur most frequently. Taking into account this fact and the specificity of FSBSI "Marine Hydrophysical Institute of RAS", when studying natural disasters the attention was focused on extreme events occurring in the marine environment. The range of issues under study [1] was quite wide: storm winds and waves [2, 3], surge fluctuations [4], tsunamis [5], seiches [6], harbor seiche and abnormal waves [7], risk of hydrogen sulphide contamination, etc. The aim of these research was not to duplicate regularly performed assessments of hazardous hydrometeorological phenomena based on traditional methods of hydrometeorological network data analysis, but to expand and supplement them. Some results of the work in this direction, which were discussed with S.F. Dotsenko repeatedly and in detail, are summarized below.

Storm winds over the Black Sea open part. The characteristics of the Black Sea coast storm winds have been studied well enough from the data of coastal hydrometeorological stations in the northern part of the sea [2, 8]. The assessments of wind field characteristics over the open part of the sea are much more uncertain

due to the lack of regular direct measurements. Satellite scatterometry is a promising type of observation but the length of measurement series with the increased accuracy is still insufficient for climatic assessments. Therefore, the main sources of information for the analysis of the wind over the sea are global and regional atmospheric reanalyses.

Despite the quantitative differences, the patterns of the spatial distribution of the storm wind (> 15 m/s) frequency over the Black Sea water area (obtained from different sources) have similar qualitative features (Fig. 1). In the western and northeastern parts of the sea storm situations occur most frequently, southeastern part is least subjected to the storms.

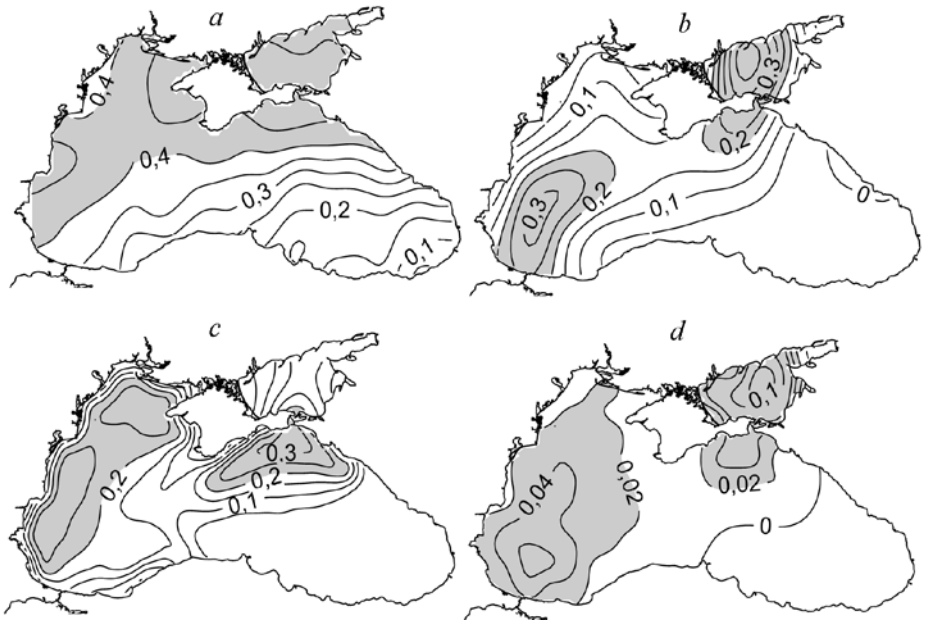

Fig. 1. Average probability (%) of storm winds (>15 m/s) according to different sources: *a* – synoptic maps [9]; *b* – ERA-40; *c* – OAI MHI [10]; *d* – MERRA

Storm wind velocity increase over the Black Sea is mainly due to cyclonic activity. Localization of the maximum storm activity values near the Kerch Strait is related to frequent passage of Mediterranean cyclones through the Asia Minor and the southern part of the Black Sea. Storm winds are of northern and northeastern directions at that weather pattern. In the western part of the sea several types of synoptic situation development lead to the massive storms. If the Mediterranean cyclones move the west part of the Black Sea or the cyclones from the Scandinavian region move to the Balkans, then the storms of the southern and southwestern directions occur. When the Atlantic cyclones move to the south of Ukraine, western and northwestern directions of the storm winds become the dominant ones. It should be pointed out that there are the processes of strong wind occurrence which are not registered at the synoptic maps and are not realized in the atmospheric models. In the first instance this applies to the Caucasian

coast where (according to the remote probing) a narrow zone of coastal storm winds (like mountain-valley circulation) may occur.

Annual average cycle of storms in the Black Sea can be divided into three seasons: autumn-winter season from October to March when the number of days with storm wind reaches its maximum (6–9 per month) and the northern and northeastern wind directions are the dominant ones (20–25% of the total number of storms); summer season from May to August with a minimum number of days with storm wind (0.5–1 per month) and the western wind direction is the dominant one (20%); transition period in April and September, when the number of days with a storm wind is 2–4 ones per month and the winds of the northern sector prevail. For all seasons the lowest frequency (repeatability) remains for storm winds of southeastern direction (< 2%) which is due to the prevailing trajectories of cyclones. Despite the fact that the storm activity in the region is subjected to significant inter-annual variability, there are no obvious changes in the seasonal variability structure of storms for the Black Sea, except for seasonal course amplitude decrease.

It should be pointed out that the coastline configuration leads to the fact that climatic characteristics of the storm wind and sea heaving often do not correspond to each other. Particularly, the most frequently occurring storms of the northern and northeastern directions cause the maximum sea heaving near the coasts of Bulgaria and Turkey. The storms of southwestern direction (such as the ones that took place in November 1981 and 2007) pose the greatest danger for navigation near the northern coast of the sea. Significant sea heaving develops near the Southern coast of the Crimea at the storm winds of the southern and southeastern directions.

The trends of the long-term storm activity variability (according to the data from coastal stations) indicate a general trend of storm activity decrease in the Black Sea over the past 50 years, when strong and storm wind probability has decreased, on average, by two times. The overall wind velocity decrease was accompanied by a reduction in the probability of moderate (6–9 m/s) and strong (≥ 10 m/s) winds and a significant increase in the frequency of weak (2–5 m/s) winds. Since the beginning of the XXI century in certain areas of the sea and the coast the wind velocity increase has begun again.

For data obtained in the open part of the sea long-term trends are not as pronounced as for the coastal stations. The graph of annual average storm wind frequency is given in Fig. 2, a separated vertical axis corresponds to each source of information. Strong wind probability decrease after the 1970s is most pronounced in ERA-40 reanalysis and in the array of synoptic maps [9]. The decrease of number of storms in this period is mostly due to reduction of northern and northeastern winds. If we consider the seasonal component of inter-annual wind velocity variability, the key role in it is played by sustainable reduction in the number of storms in winter. In other seasons the decrease of average wind velocity and strong wind probability is not so obvious and often it is statistically insignificant.

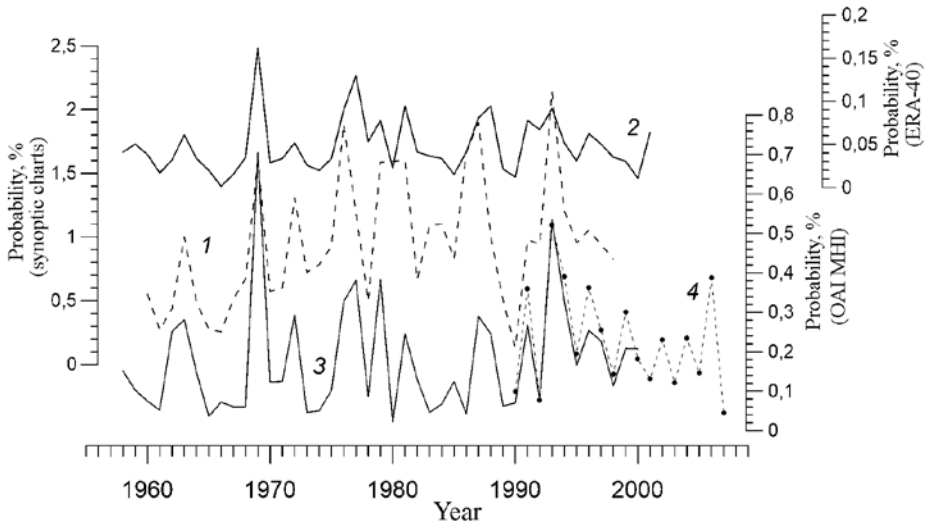

Fig. 2. Annual average values of storm wind (> 15 m/s) frequency over the Black Sea according to different sources: *1* – synoptic maps [9]; *2* – ERA-40; *3* – OAI MHI / *ERA*-40 [10]; 4 – OAI MHI / ERA-interim

The decrease of storm activity in the Black Sea which took place in 1960–1990s was due to reduction of total amount and intensity of the passing cyclones. It was also accompanied by well pronounced increase of the North Atlantic and East Atlantic Oscillations. After the 1990s the mentioned indices of large-scale atmospheric circulation have a negative trend and in this relation one may expect the increase of number of storms in the Black Sea.

Modeling of the surge processes in the Azov Sea. In [11, 12], on the basis of ADCIRC numerical hydrodynamic model [13] surge oscillations the Azov Sea level and associated processes of flooding and drainage of the Don delta were studied. Particularly, it was found that the most intensive delta flooding occurs at the western and southwestern winds. Flooding process begins at wind velocities of at least 15 m/s.

Some new results concerning the features of water level surge oscillations in the Don delta generated by the moving cyclones and the comparison of river runoff and wind surge contributions to the Don delta flooding are represented below. The modeling was carried out on unstructured grid which includes the Azov Sea and the Kerch Strait. Free passage condition was applied on the southern boundary of the strait. Grid characteristics and selection of ADCIRC model parameters are described in [11, 12].

At first the generation of surge oscillations of level and the processes of the Don delta flooding-drainage by moving anticyclone with no regard to the river runoff were studied. Wind velocity in the cyclone was determined by the gradient wind formula

$$W_g = \left[\frac{r}{\rho_a} \frac{dP_A}{dr} + \left(\frac{fr}{2} \right)^2 \right]^{1/2} - \frac{fr}{2}, \quad (1)$$

where $r = \sqrt{r_x^2 + r_y^2}$ is the distance from the center of anticyclone (x_c, y_c) to the point (x, y) in which W_g is calculated; $r_x = x - x_c$; $r_y = y - y_c$; ρ_a is air density; f is Coriolis parameter. Atmospheric pressure P_A in the formula (1) was determined by the expression

$$P_A = \begin{cases} P_0 - \delta P_A \cos^2\left(\dfrac{\pi r}{2R} \right) & \text{at } r \le R \\ P_0 & \text{at } r > R \end{cases}. \quad (2)$$

Here P_0 is a background value of atmospheric pressure; δP_A is a pressure drop between the center and periphery of cyclone; R is a radius of cyclone. According to the assessments given in [14], R = 300 km, δP_A =15 hPa.

Taking into account the expressions (1), (2) the components of wind velocity vector in the near-ground atmospheric layer were determined by the following formulas ($\alpha = 90° + \gamma$):

$$W_x = -\frac{\mu W_g}{r}(r_x \sin\alpha + r_y \cos\alpha), \; W_y = \frac{\mu W_g}{r}(r_x \cos\alpha - r_y \sin\alpha). \quad (3)$$

In the formulas (3) it is assumed that in the near-water layer the wind deviates from the tangent lines to the isobars by γ angle (which makes up 20°) counterclockwise due to the friction and its velocity is lower than the one of gradient wind. This fact is taken into account by the coefficient μ = 0.7.

In order to assess the flooded area of the delta (*FI*) and mean sea level in the delta (*SL*) the following expressions were used:

$$FI(t) = 100\% \left(1 - \frac{S(t)}{S(0)} \right), \quad SL(t) = \frac{\iint\limits_{\Omega} \eta(x,y,t)\delta_w(x,y,t)dxdy}{\iint\limits_{\Omega} \delta_w(x,y,t)dxdy}, \quad (4)$$

$$S(t) = \iint\limits_{\Omega} \delta_d(x,y,t)dxdy, \quad \delta_d(x,y,t) = \begin{cases} 1, & H(x,y,t) \le H_{\min} \\ 0, & H(x,y,t) > H_{\min} \end{cases},$$

$$\delta_w(x,y,t) = \begin{cases} 0, & H(x,y,t) \le H_{\min} \\ 1, & H(x,y,t) > H_{\min} \end{cases}.$$

Here $S(t)$ value is the land area in t moment of time; $S(0)$ is the land area in the initial moment of time; $H = h(x, y) + \eta(x, y, t)$ is a dynamic depth of the basin; h is sea depth; η is sea level deviation from the unperturbed state; $H_{\min}$ = 0.1 m is the minimum depth in the flooding-draining algorithm of ADCIRC model. In the ex-

pressions (4) the integration is performed over a rectangular region $\Omega = \{39.0°\text{E} \le x \le 39.63458°\text{E};\ 46.5°\text{E} \le y \le 47.28910°\text{N}\}$ which includes the Don delta.

In the first cycle of numerical experiments it was assumed that the cyclone moves along the zonal trajectory: $x_c = x_0 + ct$; $y_c = y_0$, where $x_0 = 29.25°$ E, $y_0 = 46.25°$ N. The velocity of the cyclone movement c took the following values: $c_1 = 20$ km/h; $c_2 = 30$ km/h; $c_3 = 40$ km/h. Total integrating time made up 72 h.

The dependencies of $\left(W = \sqrt{W_x^2 + W_y^2}\right)$ velocity and (D) wind direction on time in the point (which is located at the external boundary of the Don delta) with (x_d, y_d) = (39.375° E, 47.175° N) coordinates are given in Fig. 3, *a b*. *D* values are counted off from *x* axis which is directed to the east counterclockwise. Wind velocity curves have two maximums: the first occurs when the cyclone comes to the delta and the second – when the cyclone leaves its limits. The total time of the cyclone effect on the delta (t_d) is a time interval during which in (x_d, y_d) point $W > 0$ condition is satisfied. As it can be seen, t_d decreases with the cyclone movement velocity increase and its value makes up 27 h for $c = c_1$; 18 h for $c = c_2$; 14 h for $c = c_3$. As the cyclone passes over the delta the wind subsequently changes its direction from the southeastern to the eastern and then to the northern one. Such wind direction changes result in the mean level decrease which can be observed at *SL* curves (Fig. 3, *c*). The maximum level decreases reach the following values: –1.05 m for $c = c_1$; –0.74 m for $c = c_2$; –0.69 m for $c = c_3$. According to Fig. 3, *d*, the delta drainage due to total level decrease reaches 16–27%.

In the next cycle of calculations the point has $y_0 = 47.50°$ N coordinate (the center of the cyclone moves along the Gulf of Taganrog). In the case under consideration, the wind velocity difference between the maxima and minima makes up ~ 10 m/s (Fig. 4, *a*). Wind direction changes from the southern and southwestern to the northwestern one (Fig. 4, *b*). In the delta level elevations (rises) generated by the cyclone make up ~ 0.9 m (Fig. 4, *c*) and *FI* value does not exceed 3.5% (Fig. 4, *d*). This means that at such cyclone trajectory the flooding of the delta is insignificant.

The results of calculations at $y_0 = 48.50°$N showed that surge height in the delta increased by 1.5–2 times (Fig. 5) in comparison with the previous calculation (at $y_0 = 47.50°$N). Moreover, at $c = c_1$ significant delta flooding took place (*FI* ~ 70%). Thus, the most favorable conditions for the occurrence of extreme storm surges in the Gulf of Taganrog (resulting in significant flooding of the Don delta) occur in those cases when the cyclone affects the sea basin by its southern periphery.

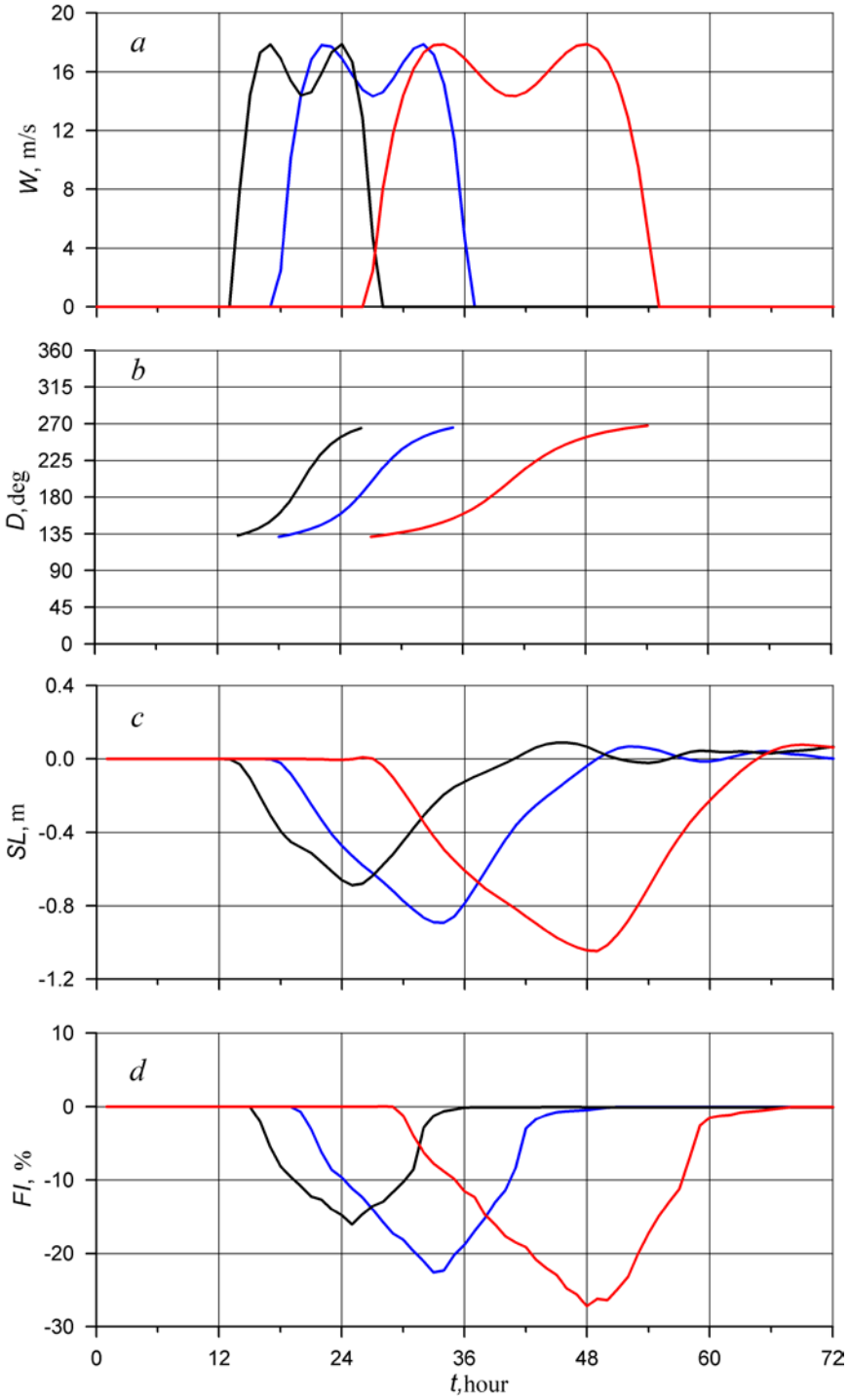

Fig. 3. Dependences of wind velocity and direction, mean water level and the Don delta flooded area on the time at R = 300 km, δP_A =15 hPa, x_0 = 29.25° E, y_0 = 46.25° N. Red curves – c = 20 km/h; blue curves – c = 30 km/h; black curves – c = 40km/h

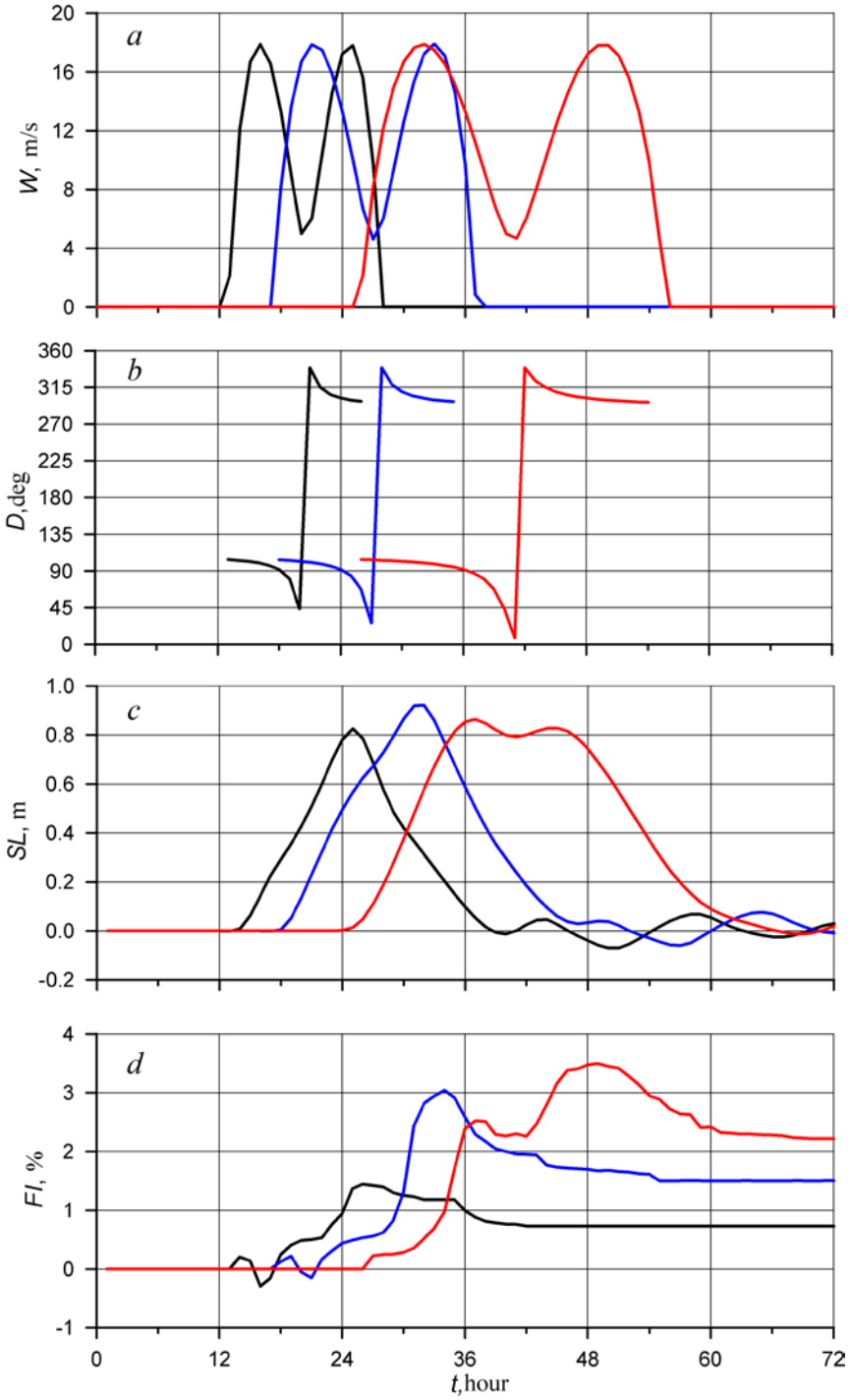

Fig. 4. Dependences of wind velocity and direction, mean water level and the Don delta flooded area on the time at R = 300 km, δP_A = 15 hPa, x_0 = 29.25° E, y_0 = 47.50° N. The correspondence of the curve colors is the same as in Fig. 3

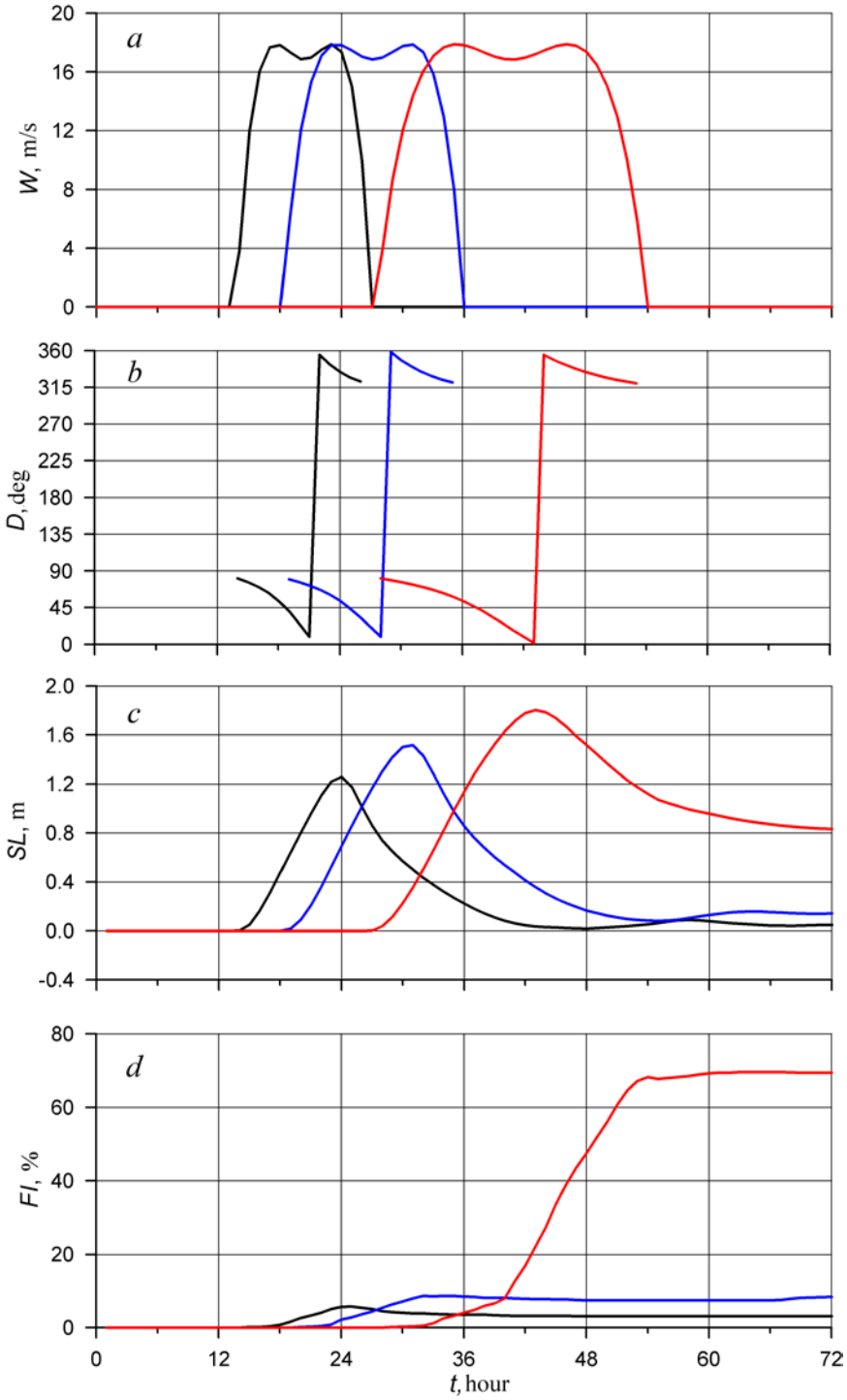

Fig. 5. Dependences of wind velocity and direction, mean water level and the Don delta flooded area on the time at R = 300 km, δP_A = 15 hPa, x_0 = 29.25° E, y_0 = 48.50° N. The correspondence of the curve colors is the same as in Fig. 3

It is of interest to obtain the assessments of river runoff contributions and wind surge to the Don delta flooding. It should be pointed out that two differently directed mechanisms exist in the delta. On the one hand, river runoff increases the overall water level in the delta. On the other hand, river discharge directed to the west reduces the velocity of surge currents. Therefore, it is quite difficult to present even a qualitative picture of the processes taking place in the delta.

In the first cycle of numerical experiments an objective was to assess the value of Don water discharge at which a significant flooding of its delta occurs. The calculations were carried out with different values of Q water discharge assuming the absence of the wind. Water discharge for the first 12 h linearly increased from zero to its maximum value and then it remained constant. Total integrating time made up 168 h.

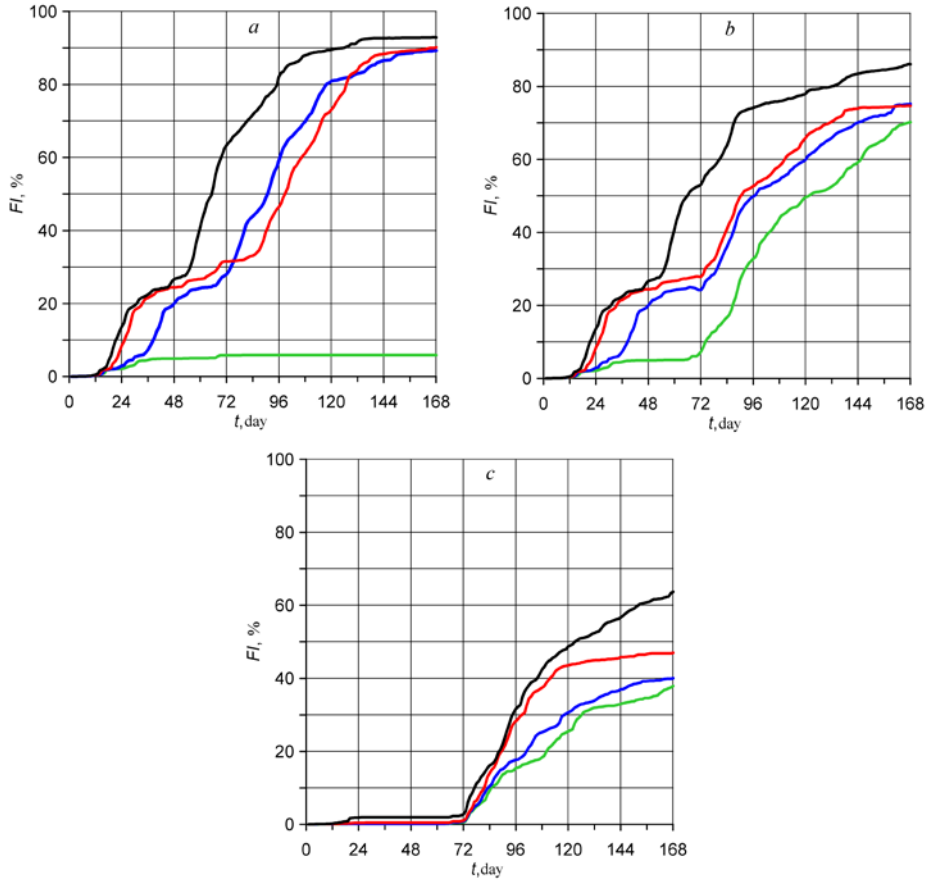

Fig. 6. Dependence of the Don delta flooded area on time at different water discharges: *a* – with no regard to wind surge: green curve – Q =1600 m^3/s, blue curve – Q =1700 m^3/s, red curve – Q =1800 m^3/s, black curve – Q = 2000 m^3/s; *b* – taking into account the wind surge: green curve – Q =1600 m^3/s, blue curve – Q =1700 m^3/s, red curve – Q =1800 m^3/s, black curve – Q = 2000 m^3/s; *c* – taking into account the wind surge: green curve – Q = 400 m^3/s, blue curve – Q = 700 m^3/s, red curve – Q = 1000 m^3/s, black curve – Q = 1400 m^3/s

As is shown by the results of *FI* parameter (Fig. 6, *a*) calculation, the process of the delta flooding at a high water (with the absence of wind surge) have a non-uniform stepped character. Avalanche-like increase of the flooded area begins from *FI* > 30% values. Total flooding (*FI* > 80%) takes place at *Q* values that exceed $Q_* = 1600$ m^3/s. This is about twice as much as the value of the Don mean discharge in a warm season [15]. For the overall delta flooding $Q > Q_*$ condition should be satisfied for at least 4–6 days.

In the next series of numerical experiments wind-induced surge was taken into account in addition to *Q*. The calculations were carried out according to the following scenario. During the first 12 h *Q* value linearly increased from 0 to its maximum and then remained constant. After 3 days of river runoff effect the wind with $D = 30°$ direction was included. At 72–84 h time interval *W* wind velocity increased from 0 to 15 m/s and then remained constant.

The graphs of the Don delta flooded area at $W = 15$ m/s for $Q \geq Q_*$ typical values are given in Fig. 6, *b*. As is obvious, after including the wind ($t > 72$ h) at $Q = Q_*$ the increase of flooding area from 6% to 70% occurs in four days. At $Q > Q_*$ the decrease of the delta flooding area by 8–14% compared to the case with no wind surge takes place. The graphs of the Don delta flooding area at $W = 15$ m/s for the $Q < Q_*$ typical values are given in Fig. 6, *c*. It can be seen in this figure that with *Q* value increase from 400 to 1400 m^3/s the delta flooding area monotonically increases from 37 to 64%.

It is possible to provide the following interpretation of the obtained modeling results. There is a certain threshold value $Q \sim Q_*$ depending on the bottom and the Don delta land morphometry features. At $Q < Q_*$ wind surge exerts a blocking effect on the river waters which promotes a more rapid water level increase in the delta arms and its spreading over the delta lowlands. At $Q > Q_*$ a part of river waters flows from the delta into the sea (due to the higher velocity of discharge currents) which causes a certain water level reduction in the delta and the decrease of its flooding area.

The results of numerical modeling showed that atmospheric cyclones propagating with 20–40 km/h velocity are the effective generators of storm surges in the Azov Sea. The intensity of surges is largely determined by the trajectory of the cyclones. Significant level rises in the Gulf of Taganrog and the Don delta occur in those cases when the trajectory of the cyclone center is above the northern boundary of the sea by ~ 2.5–3°, i.e. when the cyclone affects the sea water area by its southern periphery generating an intensive wind of western and southwestern directions.

All other things being equal, the decrease of the cyclone movement velocity causes an intensification of storm surges in the Gulf of Taganrog and the increase of delta flooded area. With a decrease in the cyclone movement velocity from 40 to 20 km/h, the flooded area increases by ~ 1.5–2 times.

The contribution of river runoff and wind surges to the flooding of the Don delta has been studied. A certain threshold value of the Don discharge $Q_* \sim 1600$ m^3/s is revealed. When the water discharge is $Q \le Q_*$ wind surge exerts a blocking impact on the river waters which promotes the water level rise in the arms and its spreading over the delta lowlands. If $Q > Q_*$, a part of the river waters flows to the sea from the delta due to intensive discharge. This results in a certain decrease of water level in the delta and reduction of flooded area.

The system for the tsunami wave evolution forecasting in the Black Sea basin. Tsunami is a dangerous natural phenomenon which is a system of long surface gravity waves caused by relatively short-term external disturbances of natural and technogenic origin. Earthquakes, underwater earthquakes, explosions of volcanoes, collapses of rocks, underwater landslides and atmospheric effects (meteotsunami) are the natural sources of such waves. The coastal and island regions of the Pacific and Indian Oceans, the Mediterranean Sea, the Eastern Atlantic, the Caribbean and some other areas of the World Ocean are the most exposed to strong tsunamis. The frequency and intensity of tsunami-type waves in the Black Sea is much lower but, according to historical reports, these waves were observed along the entire coast of the Black Sea. Most of the events were caused by the earthquakes with an epicenter in the sea; some were generated by the earthquakes at the land; meteotsunamis were also observed (for example, an event that took place near Odessa on June 27, 2014). Over the past two thousand years 22 events were recorded in the region [16, 17], eight of them were of catastrophic character and were accompanied with 2–3 m height waves. Only four of them were recorded instrumentally: June 26, 1927 and September 11, 1927 the events located to the southwest and to the south from the Southern Coast of the Crimea, December 26, 1939 with the epicenter at the land (150 km from the northeastern coast of Turkey) and July 12, 1966 in the Anapa region near the Black Sea eastern coast. With such a small amount of observational data, numerical modeling becomes the only instrument for tsunami research in the region.

The first version of the system for tsunami evolution forecast in the Black Sea was developed for the preliminary assessment of the tsunami hazard of the Black Sea coast, extreme sea level rises and decreases in the coastal zone, to study the tsunami characteristics and features of their distribution. The basis of this system is the computer implementation of barotropic nonlinear evolutionary model of long waves with regard to the quadratic bottom friction [18, 19]. The computational grid with 1000 m spatial step was applied in the system. Simulation foci of elliptical tsunami were located in high-risk earthquake zones (Fig. 7). Initial level shift was set to be of constant sign. The parameters of seismic sources were determined depending on the earthquake magnitude M: the dimensions of the elliptical generation zone were determined by generalized empirical relationships for the Eurasian region [20] and the maximum sea level shift in the epicenter – by the empirical formula given in [21].

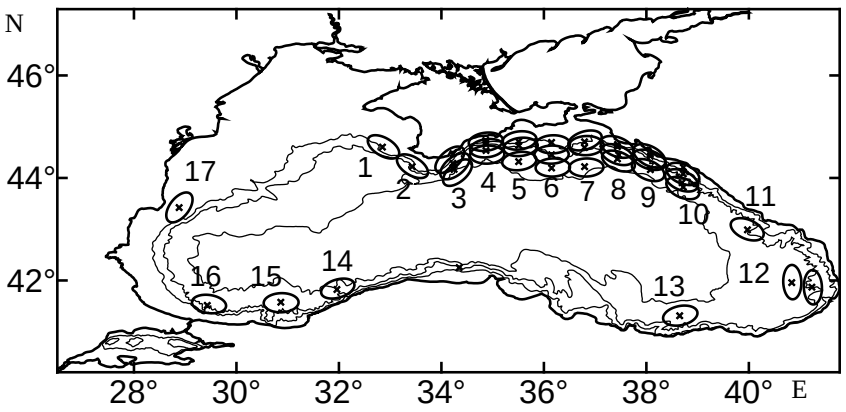

Fig. 7. Computational domain and location scheme of model seismic sources

Particularly, for M = 7 magnitude the length of the major axis of the ellipse is 50.1 km, the one of the minor axis is 29.5 km; the maximum sea level shift in the seismic source is 1 m. Figures *3–10* (Fig. 7) denote the groups of three seismic sources with a different distance from the coast. The centers of these sources are located on 200, 1000 and 1800 m isobaths, respectively. The calculations were carried out down to 5 m depth. The examples of tsunami wave evolution maps from the generation zone *3* for different moments of time are represented in Fig. 8.

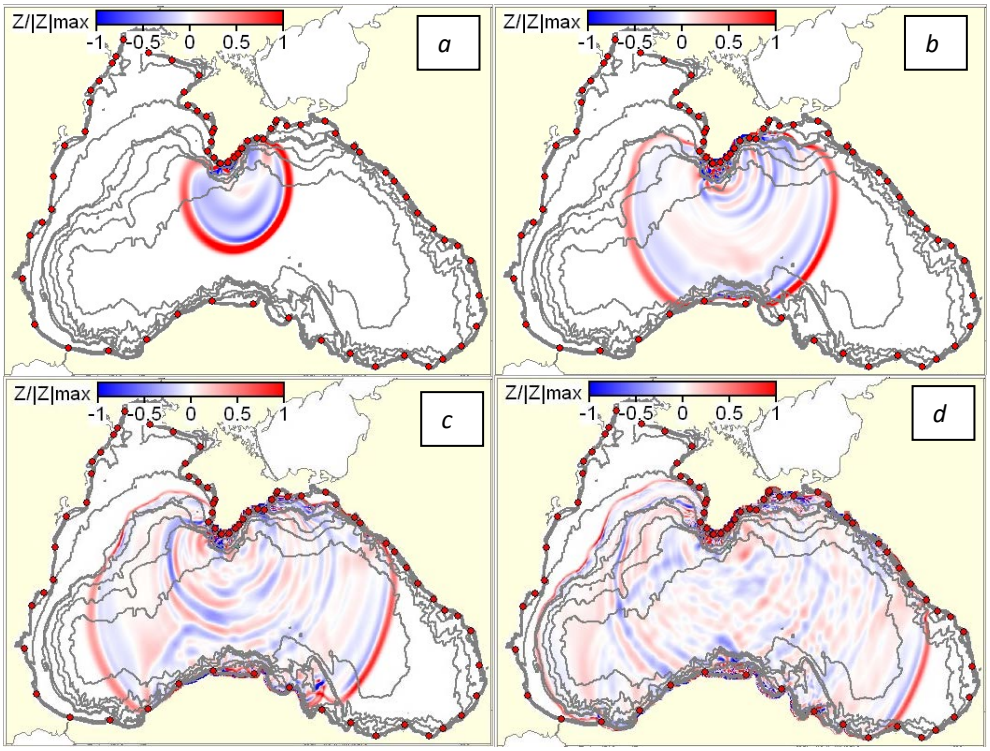

Fig. 8. The examples of tsunami evolution maps from the seismic source *3* for different moments of time: *a* – 15 min, *b* – 30 min, *c* – 45 min, *d* – 60 min

Recording of sea level oscillations was carried out in the computational grid cells located near 5 meter isobaths and forming a continuous boundary (Fig. 9, *a*). According to the results of the calculation extreme sea level rises and decreases were assessed and their distributions along this boundary (on the basis of which preliminary conclusions about the tsunami hazard of various sections of the Black Sea coast were drawn) were constructed. The conducted research showed that location of tsunami generation zones significantly affects the distribution of wave heights along the coast. At the initial stage the greatest wave heights and wave velocities are recorded in that direction which is perpendicular to the major axis of the elliptical generation zone. Further, the basin bathymetry significantly affects the wave propagation. The considered seismic sources of tsunamis are located at the continental slope, therefore in the majority of cases the most intensive waves are formed in the direction of the closest coastline section. The closer generation zone is to the shore, the more manifested is this wave feature.

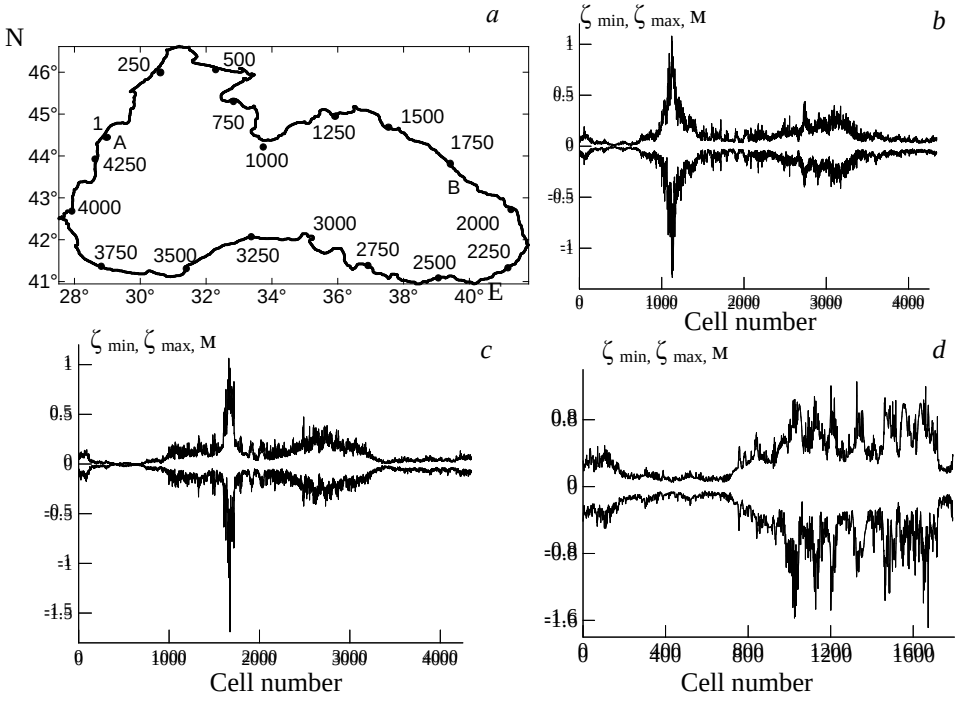

Fig. 9. Assessments of extreme sea level rises and decreases, ζ_{min}, ζ_{max}: *a* – the boundary formed by the computational domain cells in which the sea level oscillations are registered; *b, c* – distribution of the maximum sea level rises and decreases along the boundary for the sources *3* and *10*, respectively; *d* – distribution of the maximum sea level rises and decreases along the section of *AB* boundary for all seismic sources

As a rule, a wave propagating towards the abyssal part of the sea causes noticeable sea level oscillations at the opposite part of the coast (taking into account the wave refraction) (Fig. 9, *b*, *c*) which is a consequence of the fact that the basin is an enclosed one. In rare cases, the amplitude of the oscillations on the opposite sea shore and in the coastal points, which are the closest to the generation zone, can

be commensurable. From all the considered seismic sources (Fig. 9) tsunami foci located in the northeastern part of the Black Sea constitute the greatest potential danger for *AB* section of the Black Sea coast (Fig. 9, *a*) (Crimean-Caucasian seismically active area). The northwestern part of the sea is characterized by lower tsunami hazard. For the northwestern part of the coast extreme sea level rises and decreases (by the absolute magnitude) are significantly smaller than the maximum level shift in the tsunami generation zone. The greatest wave intensification was recorded at the section from the Southern Coast of the Crimea to *B* point (Fig. 9, *a*). Significant sea level oscillations in a series of points of the Southern Coast of the Crimea are also possible due to the capture of waves propagating from *13–17* foci towards northwest, north and northeast.

The works on the Black Sea coast tsunami hazard are continued, certain coastline sections are considered using the grids with higher resolution, the features of tsunami wave propagation in the Black Sea bays and gulfs [22, 23] are studied (also with regard for the wave uprush onto a shore).

Conclusion. Storm situations occur most often in the western and northeastern parts of the Black Sea in autumn-winter season from October to March with the predominance of winds of northern and northeastern directions. The decrease of storm activity in the Black Sea that took place observed in the end of the XX century was due to diminution of total amount and intensity of the passing cyclones. Due to long-term tendencies of the North Atlantic Oscillation and the East Atlantic Oscillation atmosphere indices, future increase of the storm amount in the Black Sea would be expected.

The effective sources of storm surges in the Sea of Azov are the atmospheric cyclones spreading with 20–40 km/h velocity. Cyclone movement velocity decrease results in a storm surge intensification in the Gulf of Taganrog and increase of the flooded area in the Don delta. When the Don discharge becomes lower than the threshold value ~1600 m^3/s, the wind surge exerts a blocking impact upon the river water that promotes the sea level rise in the delta arms and lowlands.

The highest potential tsunami hazard for the Black Sea northern coast is represented by the earthquake epicenters located in the Crimea – Caucasus seismic zone. Tsunami hazard in the northwestern part of the sea is significantly lower.

Acknowledgements. The work is carried out within the framework of the State Order No. 0827-2015-0001 "Fundamental Research of the Processes in the Ocean-Atmosphere-Lithosphere System which Determine Spatial-Temporal Environment Variability and Global and Regional Climate" ("Climate" code) and No. 0827-2014-0010 "Complex Interdisciplinary Studies of Oceanographic Processes Determining the Functioning and Evolution of the Black and Azov Sea Ecosystem on the Basis of Modern Methods of Control of the Marine Environment and Grid Technologies".

REFERENCES

1. Dotsenko , S.F. and Ivanov, V.A., 2010. *Prirodnye Katastrofy Azovo-Chernomorskogo Regiona* [Natural Catastrophes of the Azov-Black Sea Region]. [e-book] Sevastopol: ECOSI-Gidrofizika, 174 p. Available at: http://meteo.geofaq.ru/books/612759_D9E3D_docenko_s_f_ivanov_v_a_prirodnye_katastrofy_azovo_chernomors.pdf [Accessed 20 December 2016] (in Russian).

2. Repetin, L.N. and Belokopytov, V.N., 2008. Rezhim Vetra nad Poberezh'em i Shel'fom Severo-Vostochnoy Chasti Chernogo Morya [Wind Regime over the Coast and Shelf of the Black Sea North-Eastern Part]. In: *Nauchnye trudy UkrNIGMI* [Scientific Works of UHMI]. Kiev: UHMI. Iss. 257, pp. 84-105 (in Russian).

3. Efimov, V.V. and Komarovskaya, O.I., 2009. *Atlas Ekstremal'nogo Vetrovogo Volneniya Chernogo Morya* [Atlas of Extreme Wind Waves in the Black Sea]. Sevastopol: ECOSI-Gidrofizika, 59 p. (in Russian).

4. Il'in, Yu.P., Fomin, V.V., D'yakov, N.N. and Gorbach, S.B., 2009. *Gidrometeorologicheskie Usloviya Morey Ukrainy. T. 1. Azovskoe More* [Hydrometeorological Conditions of the Seas of Ukraine. Vol. 1. The Sea of Azov]. Sevastopol, 401 p. (in Russian).

5. Dotsenko, S.F., 1994. Chernomorskiye Tsunami [The Black Sea Tsunamis]. *Izvestiya RAN. Fizika Atmosfery i Okeana,* 30(4), pp. 513-519 (in Russian).

6. Dotsenko, S.F and Miklashevskaya, N.A., 2008. Generation of Seiches by Moving Baric Fronts in Bounded Basins. *Physical Oceanography*, [e-journal], 18(2), pp. 63-77. doi:10.1007/s11110-008-9014-6

7. Dotsenko, S.F., Ivanov, V.A. and Poberezhny, Yu.A., 2009. Volny-Ubiytsy v Severo-Zapadnoy Chasti Chernogo Morya [Freak Waves in the North-Western Part of the Black Sea]. *Dopovidi NAN Ukraini*, (9), pp. 113-117 (in Russian).

8. Naumova, V.A., Evstigneev, M.P., Evstigneev, V.P. and Lyubarets, E.P., 2010. Vetro-Volnovye Usloviya Azovo-Chernomorskogo Poberezh'ya Ukrainy [Wind-Wave Conditions of the Azov-Black Sea Coast of Ukraine]. In: UHMI, 2010. *Nauchnye trudy UkrNIGMI* [Scientific Works of UHMI]. Kiev: UHMI. Iss. 259, pp. 263-283 (in Russian).

9. Belokopytov, V.N., Kudryavtseva, G.F. and Lipchenko, M.M., 1998. Atmosfernoe Davlenie i Veter nad Chernym Morem (1961–1990 gg.) [Atmospheric Pressure and Wind over the Black Sea (1961–1990)]. In: UHMI, 1998. *Nauchnye trudy UkrNIGMI* [Scientific Works of UHMI]. Kiev: UHMI. Iss. 246, pp. 174-181 (in Russian).

10. Efimov, V.V. amd Anisimov, A.E., 2011. Climatic Parameters of Wind Field Variability in the Black Sea Region: Numerical Reanalysis of Regional Atmosperic Circulation. *Izvestiya. Atmospheric and Ocean Physics*, [e-journal] 47(3), pp. 350-361. doi:10.1134/S0001433811030030

11. Fomin, V.V., Lazorenko, D.I., Alekseev, D.V. and Polozok, A.A., 2015. Shtormovye Nagony v Taganrogskom Zalive i Zatoplenie Del'ty Dona [Storm Surge in the Taganrog Bay and Flooding of the Don Delta]. In: V. A. Ivanov, ed., 2015. *Ekologicheskaya Bezopasnost' Pribrezhnoy i Shel'fovoy Zon Morya* [Ecological Safety in Coastal and Shelf Zones of the Sea]. Sevastopol: ECOSI-Gidrofizika. Iss. 1, pp. 74-82 (in Russian).

12. Fomin, V.V., 2016. Raschety Urovnya i Vetrovogo Volneniya v Taganrogskom Zalive na Osnove Sovmestnoy Modeli [Sea Level and Wind Waves Calculations in Taganrog Bay with the Use of Coupling Model]. In: SOI, 2016. *Trudy GOIN* [SOI Proceedings]. Moscow: SOI. Iss. 217, pp. 254-267 (in Russian).

13. Luettich, R.A., Westerink, J.J. and Scheffner, N.W., 1992. *ADCIRC: an Advanced Three-dimensional Circulation Model for Shelves, Coasts, and Estuaries. Report 1. Theory and Methodology of ADCIRC-2DDI and ADCIRC-3DL*. [e-book] Vicksburg, Mississippi, USA: Army Engineers Waterways Experiment Station, 141 p. Available at: http://www.unc.edu/ims/adcirc/pub-lications/1992/1992_Luettich02.pdf [Accessed 20 February 2017].

14. Grishin, G.A., Bayankina, T.M., Kalinin, E.I and Lundberg, M.M., 1991. Ob Evolyutsii Yuzhnykh Tsiklonov, Vykhodyashchikh na Chernoe More i Territoriyu Ukrainy, po Dannym Sputnikovykh i Nazemnykh Nablyudeniy [On Evolution of Southern Cyclones Entering the Black Sea and Ukraine Territory according to Satellite and Land Observations]. *Issledovaniya Zemli iz Kosmosa*, (3), pp. 89-94 (in Russian).

15. Filippov, Yu.G., 2014. Raschety Urovnya v Vostochnoy Chasti Taganrogskogo Zaliva [Calculations of a Degree in the Eastern Part of the Taganrog Bay]. In: SOI, 2015. *Trudy GOIN* [SOI Proceedings]. Moscow: SOI. Iss. 215, pp. 136-143 (in Russian).

16. Nikonov, A.A., 1997. Tsunami Occurrence on the Coasts of the Black Sea and the Sea of Azov. *Izv. Phys. Solid Earth*, 33, pp. 72-87.

17. Yalçiner, A., Pelinovsky, E., Talipova, T., Kurkin, A., Kozelkov, A. and Zaitsev, A., 2004. Tsunamis in the Black Sea: Comparison of the Historical, Instrumental and Numerical Data. *J. Geophys. Res.*, [e-journal] 109(C12), C12023. doi:10.1029/2003JC002113

18. Liu, P.L.-F., Cho, Y.-S., Briggs, M.J., Kanoglu, U. and Synolakis, C.E., 1995. Runup of Solitary Waves on a Circular Island. *J. Fluid Mech.*, [e-journal] 302, pp. 259-285. doi:10.1017/S0022112095004095

19. Dotsenko, S.F. and Integrov, A.V., 2013. Kharakteristika Voln Tsunami Seysmicheskogo Proiskhozhdeniya v Basseyne Chernogo Morya po Rezul'tatam Chislennogo Modelirovaniya [Characteristics of Seismic Origin Tsunami Waves in the Black Sea Basin according to Numerical Modeling Results]. *Morskoy Gidrofizicheskiy Zhurnal*, (3), pp. 25-34 (in Russian).

20. Ulomov, V.I., Polyakova, T.P., Shumilina, L.S., Chernysheva, G.V., Medvedeva, N.S., Savarenskaya, O.E. and Stepanova, M.B., 1993. Opyt Kartirovaniya Ochagov Zemletryaseniy [Experience in Earthquake Foci Mapping]. In: *Seysmichnost' i Seysmicheskoe Rayonirovanie Severnoy Evrazii* [Seismicity and Seismic Zoning of Northern Eurasia]. Moscow: IPE RAS. Iss. 1, pp. 99-108 (in Russian).

21. Pelinovskiy, E.N., 1982. *Nelineynaya Dinamika Voln Tsunami* [Nonlinear Dynamics of Tsunami Waves]. Gor'kiy: IPF AN SSSR, 226 p. (in Russian).

22. Dotsenko, S.F. and Sannikova, N.K.V., 2011. Analiz Osobennostey Rasprostraneniya Tsunami v Shel'fovoy Zone Basseyna [Analysis of Tsunami Propagation Features in the Shelf Zone of a Basin]. *Morskoy Gidrofizicheskiy Zhurnal*, (6), pp. 3-19 (in Russian).

23. Bazykina, A.Yu. and Dotsenko, S.F., 2016. Propagation of Tsunami-Like Surface Long Waves in the Bays of a Variable Depth**.** *Physical Oceanography*, (4), pp. 3-12. doi:10.22449/1573-160X-2016-4-3-11